Available online at www.sciencedirect.com
ScienceDirect
Geomorphology 97 (2008) 274–286
GEOMORPHOLOGY
www.elsevier.com/locate/geomorph

Rates of fluvial bedrock incision within an actively uplifting orogen: Central Karakoram Mountains, northern Pakistan

Yeong Bae Seong [a,1], Lewis A. Owen [a,*], Michael P. Bishop [b], Andrew Bush [c], Penny Clendon [d], Luke Copland [e], Robert C. Finkel [f], Ulrich Kamp [g], John F. Shroder Jr. [b]

[a] Department of Geology, University of Cincinnati, P.O. Box 0013, Cincinnati, OH 45221-0013, USA
[b] Department of Geography and Geology, University of Nebraska — Omaha, 6001 Dodge Street, Omaha, NE 68182-0199, USA
[c] Department of Earth and Atmospheric Sciences, University of Alberta, 1-26 Earth Sciences Building, Edmonton, Alberta, Canada T6G 2E3
[d] Department of Geography, University of Canterbury, Private Bag 4800 Christchurch, New Zealand
[e] Department of Geography, University of Ottawa, 60 University, Ottawa, Ontario, Canada K1N 6N5
[f] Center for Accelerator Mass Spectrometry, Lawrence Livermore National Laboratory, Livermore, California, 94550, USA
[g] Department of Geography, The University of Montana, SS 204, Missoula, MT 59812-5040, USA

Received 30 March 2007; received in revised form 14 August 2007; accepted 16 August 2007
Available online 30 August 2007

Abstract

Terrestrial cosmogenic nuclide (TCN) ^{10}Be surface exposure ages for strath terraces along the Braldu River in the Central Karakoram Mountains range from 0.8 to 11 ka. This indicates that strath terrace formation began to occur rapidly upon deglaciation of the Braldu valley at ~11 ka. Fluvial incision rates for the Braldu River based on the TCN ages for strath terraces range from 2 to 29 mm/a. The fluvial incision rates for the central gorged section of the Braldu River are an order of magnitude greater than those for the upper and lower reaches. This difference is reflected in the modern stream gradient and valley morphology. The higher incision rates in the gorged central reach of the Braldu River likely reflect differential uplift above the Main Karakoram Thrust that has resulted in the presence of a knickpoint and more rapid fluvial incision. The postglacial fluvial incision rate (2–3 mm/a) for the upper and lower reaches are of the same order of magnitude as the exhumation rates estimated from previously published thermochronological data for the Baltoro granite in the upper catchment region and for the adjacent Himalayan regions.

Keywords: Fluvial incision rates; Terrestrial cosmogenic nuclide (TCN) surface exposure dating; Strath terraces; Topography

1. Introduction

Over the last decade, much debate has occurred about the nature of the feedbacks between tectonics and surface processes in the landscape evolution of actively deforming mountain belts (Burbank et al., 1996; Brozovic et al., 1997; Zeitler et al., 2001). The upward flux of bedrock from tectonics and isostasy and the outgoing mass flux through surface processes generate relief and dictate landscape morphology across tectonically active regions. Thus the fluvial system, which actively responds to uplift, can be used as a proxy to identify actively uplifting regions (Seeber and Gornitz,

* Corresponding author.
E-mail address: Lewis.Owen@uc.edu (L.A. Owen).
[1] Current address: Department of Earth and Environmental Sciences, Korea University, Anam-Dong, Seongbuk-Gu, Seoul, 136-704, Korea.

0169-555X/$ - see front matter © 2007 Published by Elsevier B.V.
doi:10.1016/j.geomorph.2007.08.011

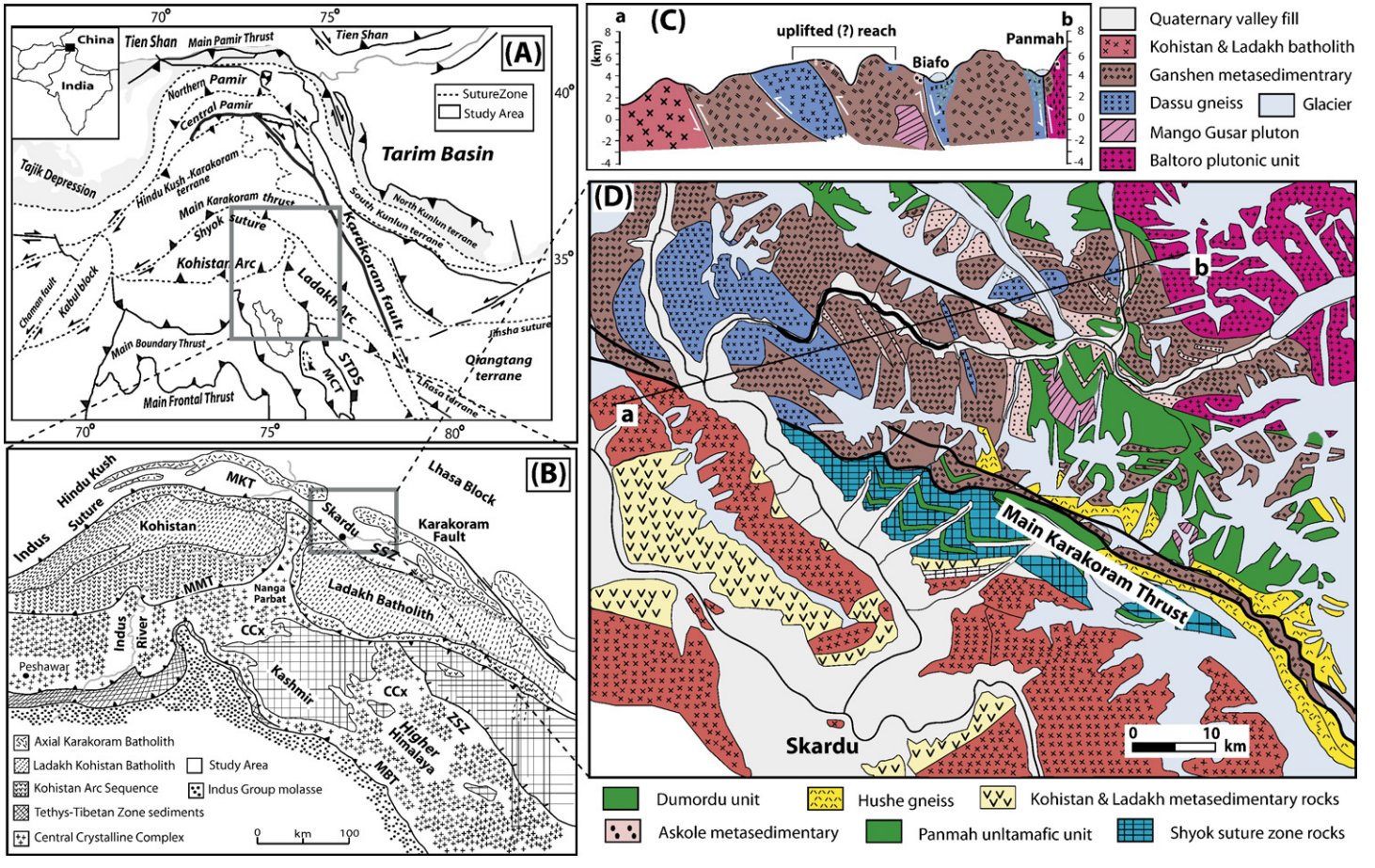

Fig. 1. Geologic content of the study area. (A) Tectonic map of the western end of the Himalayan-Tibetan orogen (modified from Robinson et al., 2004; STDS—South Tibetan Detachment, MCT—Main Central Thrust). (B) Geologic map of the central Karakoram (after Parrish and Tirrul, 1989; MBT—Main Boundary Thrust; CCx—Central Crystalline Complex of Higher Himalaya; ZSZ, Zanskar Shear Zone; MMT—Main Mantle Thrust; MKT—Main Karakoram Thrust; SSZ—Shyok Suture Zone; AKB—Axial Karakoram Batholith, and BG—Baltoro Granite). (C) Cross section from Mungo and Biafo (adapted from Searle, 1991). The location of the cross section is shown in part D. (D) Geologic map of the Central Karakoram (after Searle, 1991).

1983; Zhang, 1998; Kirby and Whipple, 2001; Finlayson et al., 2002; Montgomery et al., 2002; Montgomery, 2004; Safran et al., 2005). Consequently, fluvial characteristics, such as longitudinal stream profiles and incision rates, can be used to help define the spatial distribution and relative magnitude of surface uplift.

This paper focuses on defining rates of fluvial incision along one of the most impressive mountain valley systems in the world, the Braldu–Shigar River system of the Central Karakoram Mountains in northern Pakistan. This river system drains the Baltoro Glacier system and adjacent glaciers that originate in the world's highest topography, home of K2, the world's second highest mountain (Fig. 1). The paper also explores the relationship between tectonic and surface erosional processes along the Braldu–Shigar River system. Terrestrial cosmogenic nuclide (TCN) ^{10}Be exposure ages are used to determine fluvial incision rates from abandoned river-cut terrace straths. In addition, topographic analysis of digital elevation models (DEMs) is used to characterize the landscape.

2. Study area

The Central Karakoram Mountains are situated at the western end of the Transhimalayan Mountains and are the result of the Indian–Asian continental–continental collision (Searle, 1991; Fig. 1). The region contains some of the world's highest peaks and longest glaciers, as well as a portion of one of the world's largest rivers (the Indus River; Fig. 2). Furthermore, the region is still rapidly

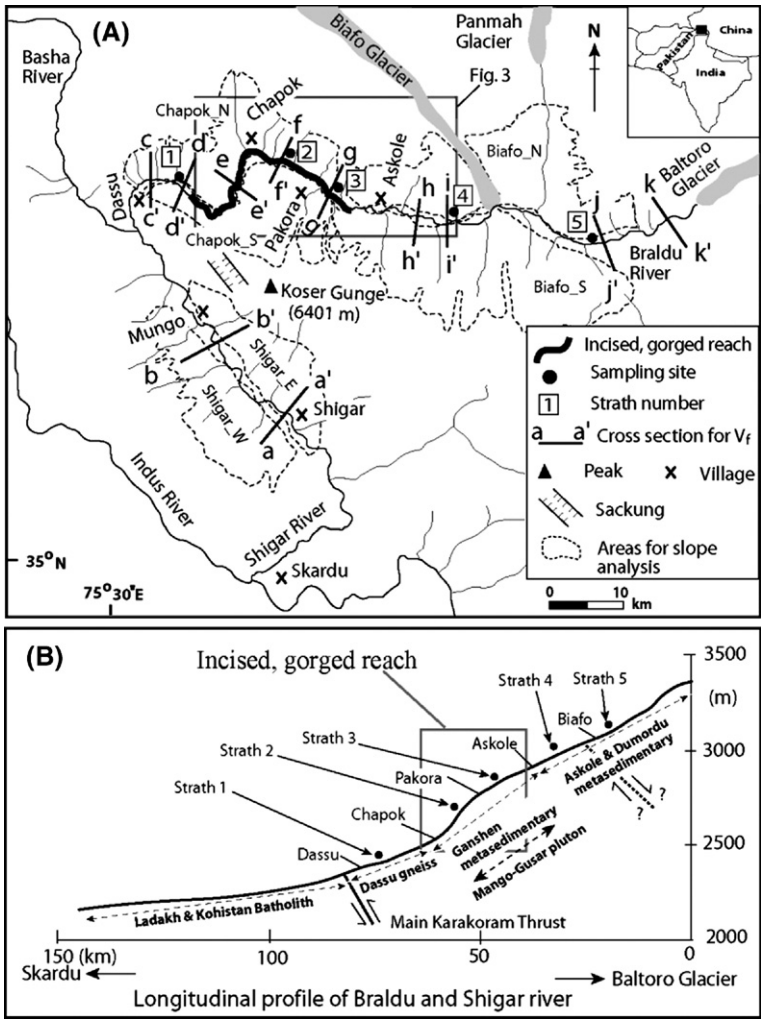

Fig. 2. The Braldu–Shigar River study area showing (A) the drainage system and locations of sampling site and (B) the longitudinal profile of Braldu–Shigar River from the snout of the Baltoro glacier to the Skardu basin. The locations, height above the present river, ages, incision rates, and numbers of dated strath terraces are shown. Incision rates are highest in the middle, incised, gorged reach around Chapok.

uplifting and is being intensely denuded (Foster et al., 1994). This dynamic tectonism results in the Central Karakoram Mountains being the highest mountain belt on Earth with >70 peaks rising above 7000 m above sea level (asl) and four peaks exceeding 8000 m asl. The intense denudation produces some of the greatest relative relief on our planet, with valley floors averaging 2000 m asl and a relative relief of >4000 m. The study region comprises medium- and high-grade metamorphic rocks, which are offset by the Main Karakoram Thrust (MKT) that trends SE across the region (Fig. 1D). Foster et al. (1994) showed that in the K2 region, just to the northeast of the study area, exhumation during the last 3–5 Ma was extremely rapid (3–6 mm/a), with ≥6 km exhumation having occurred at an altitude of 6000 m asl. Although there is great potential in this region for understating the interaction between tectonic uplift and surface processes, few geomorphic studies have been performed in this mountain range because of its logistical and political inaccessibility.

Most tributary channels of the Braldu River draining the small glaciers and the snow fields are of first and second Strahler stream order (derived from a 1:100,000 scale map). The Braldu River (third order stream) is located in the northern part of the Central Karakoram Mountains and it drains from the Baltoro Glacier and other glaciers including the Biafo and Panmah. The Braldu River joins with the Basha River to form the Shigar River near Mungo at the head of the Shigar valley (Fig. 2A). Ultimately, the Shigar River merges with the Indus River (fifth order stream) at the town of Skardu.

The channel pattern of the Braldu–Shigar River system changes several times along its length, from braided to gorged sections to meandering forms, some of which are entrenched. The braided pattern of the channel dominates the upper reaches flowing from the snout of the Baltoro Glacier through an extensive outwash plain. The braided channels comprise cobbly and pebbly bars and swales. These are modified seasonally from the extremely variable stream discharges, which differ by more than an order of magnitude difference from one season to the next.

The central reach of the Braldu River is gorged, and near the village of Chapok the Braldu River cuts a deep bedrock channel and through a large landslide (Gomboro rockslide of Hewitt, 1998) that has deflected the river out of its original channel and across bedrock spurs. Here the river has cut strath terraces, rapids, and small waterfalls. The lower reaches are dominated by meanders that sweep across a wide floodplain. The longitudinal profile of the Braldu–Shigar River system can be subdivided into three zones on the basis of stream gradient and pattern and on channel form (Fig. 2B). The river's longitudinal profile is convex for its upper reach, transitional for its central reach of the gorge section, and concave for its lower reach. A major knickpoint occurs near Chapok (Fig. 2B) at the western end of the central reach of the Braldu River.

Seong et al. (in press) described the general geomorphology of the region and highlighted the importance of glacial and paraglacial processes for its landscape evolution. Furthermore, Seong et al. (submitted for

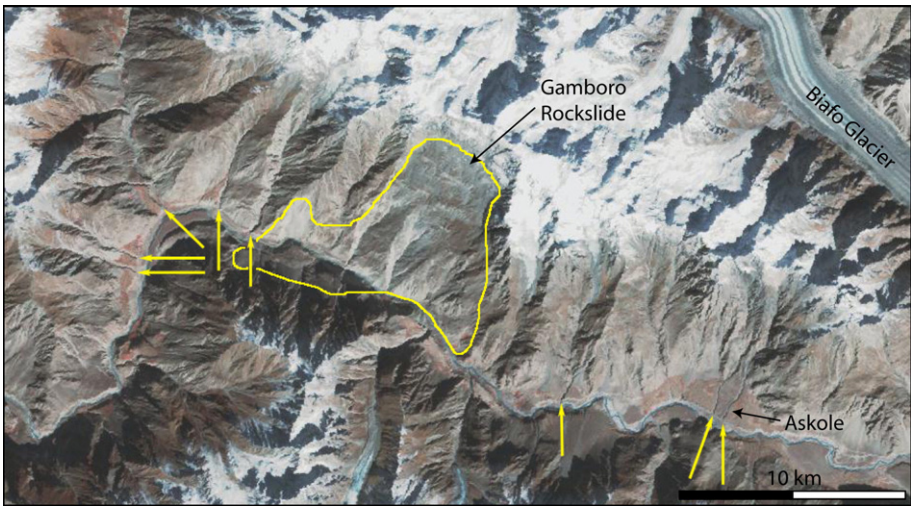

Fig. 3. Portion of Landsat 7 Enhanced Thematic Mapper Plus (ETM+) image, Worldwide Reference System 2 (WRS2) Path 149 Row 35, acquired 29 October 2000, showing the middle Braldu River gorge. The yellow arrows point to entrenched colluvial–alluvial fans, some of which are marked with a vegetation signature caused by irrigated agriculture, others of which are dry. The Gomboro rockslide is outlined in yellow in the center. North is to the top of the image.

publication) showed that the Braldu–Shigar valley was occupied by a thick (>1 km) valley glacier at least three times during the Pleistocene. The NW–SE trending MKT crosses the Braldu River at the western end of the central gorged section (Fig. 2). The relative relief in the central gorge section is ~4000 m, rising to the top of Koser Gunge at 6401 m asl (Fig. 2A). Within the central reach of the Braldu River, the stream gradient is ~13 m/km, while in the lower and upper reaches the stream gradients are 4 m/km and 8 m/km, respectively.

Both the Shigar Valley and the Braldu River Valley near the Baltoro Glacier are marked by large and small colluvial–alluvial fans that are being actively aggraded by rapid wet debris flows. Markedly, however, the central gorged reach of the Braldu River is distinguished from the other two areas by more than five colluvial–alluvial fans that are entrenched by deep (~5–15 m) erosional gorges that show these fans are no longer actively aggrading (Fig. 3). These entrenched fans occur both upstream and downstream from the large Gomboro rockslide, which shows that this landslide could not be responsible for the entrenchment, as for example could be the case where a large mass movement affected incision of the longitudinal profile once the landslide dam was breached.

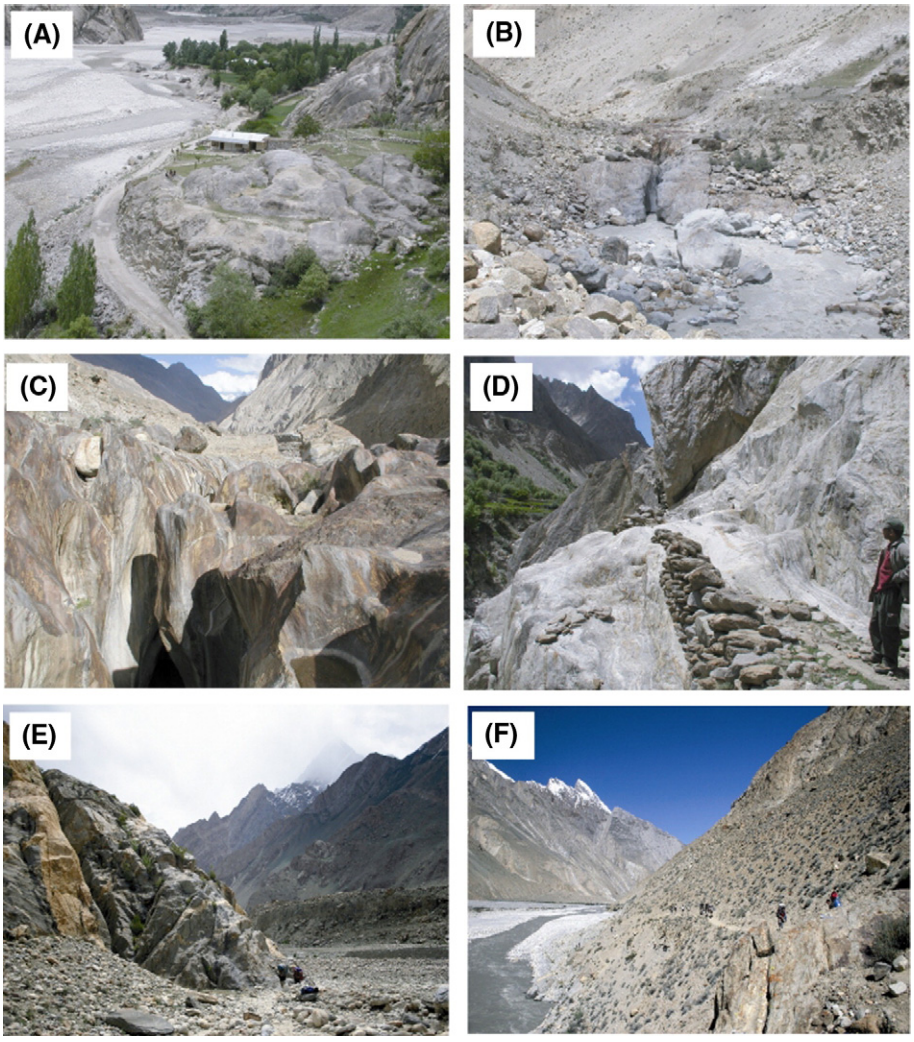

Fig. 4. Strath terraces along the Braldu River showing the sampling locations for TCN surface exposure dating. (A) View looking west at the strath terrace (#1, TCN sample K2-21) near Dassu with undulated smoothed bedrock knobs. (B) View of gorge and strath terrace (#2, TCN samples K2-42 and K2-43) around Chapok. This was recognized by Hewitt (1998) as an epigenetic gorge formed when and where the Gomboro rock slide(s) deflected the river, and (C) its closer view. These strath terraces rise 20–30 m above the present river. (D) View of rock-cut terrace (strath # 3, TCN sample K2-64) present around Pakora, illustrating a fluvially and smooth polished strath surface. (E) The strath terrace (#4, TCN sample K2-71) between Askole and Biafo, at 36 m above the present river. The thick (>5 m) gravel deposit against the terrace implies paleoriver level. (F) Strath terrace (#5, TCN samples K2-101 and K2-102) between the Biafo and Baltoro glacier.

Strath terraces are present along the Braldu River, but are rare in the Shigar valley (Fig. 4). Most of the strath terraces are unpaired or paired with fill-terraces comprising fluvial gravels. Strath surfaces are most common 20 to 40 m above the present river and are rare at higher elevations. The strath terraces range in width from 5 to 10 m and stretch for lengths of between 10 to 20 m. The surfaces of the strath terraces commonly have well-developed fluvial polishing, resulting in smooth bedrock knobs rising tens of centimeters to 2 m in height, as well as flatter areas of uneven width. All the surfaces show well-developed fluvial features (such as potholes, smooth polish, and sculpted flutes) consistent with those present within the contemporary river. The lower strath terraces (e.g., strath 1 in Fig. 2) are generally broader and longer than the higher strath terraces (e.g., strath 4 in Fig. 2).

3. Methods

3.1. Terrestrial cosmogenic nuclide (TCN) exposure dating

Strath terraces are formed when a river cuts laterally into bedrock to form a bench (Merritts et al., 1994). Subsequent vertical entrenchment causes abandonment of the strath. If the timing of the abandonment and the height of the terrace above the present river are defined, the mean incision rate of the river can be determined. The heights of strath terraces along the Braldu River were therefore measured using a hand held range finder, and they were sampled for TCN surface exposure dating to define their TCN surface exposure ages. Samples for TCN ^{10}Be surface exposure dating were collected from seven different locations on five different strath terraces (Figs. 2 and 4; Table 1). Locations where there was apparent evidence of landsliding, which would lead to a possible underestimation of the exposure age and thus an overestimation of the incision rate, were avoided as far as possible in this study. This was not entirely possible, however, in the area of the central gorge where the large Gomboro rockslide occurred. The degree of weathering and the site specific conditions for each sample location were recorded. Topographic shielding was determined by measuring the inclination from each sample site to the top of surrounding mountain ridges and peaks. The TCN ^{10}Be surface exposure dating samples were collected by hammering off a 1–5 cm layer of quartz-rich rock on top of the strath terrace at each sampling site.

All the samples were prepared in the geochronology laboratories at the University of Cincinnati. First, the samples were crushed and sieved. Quartz was then separated from the 250–500 μm size fraction using the methods of Kohl and Nishiizumi (1992). After the addition of ^{9}Be carrier, Be was separated and purified by ion exchange chromatography and precipitated at pH > 7. The hydroxides were oxidized by ignition in quartz crucibles. BeO was mixed with Nb metal and loaded onto targets for the determination of the ^{10}Be/^{9}Be ratio by accelerator mass spectrometry at the Center for Accelerator Mass Spectrometry in the Lawrence Livermore National Laboratory. Isotope ratios were compared to ICN Pharmaceutical, Incorporated ^{10}Be standards prepared by Nishiizumi et al. (2007) and using a ^{10}Be half-life of 1.5×10^{6} year. The measured isotope ratios were converted to TCN concentrations in quartz using the total ^{10}Be in the samples and the sample weights. TCN ^{10}Be concentrations were then converted to steady-state erosion rate using sea level high latitude (SLHL) ^{10}Be production rate of 4.98 atoms per gram of quartz per year (Lal, 1991; Stone, 2000; Balco et al., in press). Scaling

Table 1
Sampling locations for strath terraces, topographic shielding factors, ^{10}Be concentrations, and ^{10}Be surface exposure dates

Strath number	Sample ID	Distance downstream (km)	Latitude (±0.001N°)	Longitude (±0.001E°)	Altitude (m asl)	Height above river (m)	Shielding factor	^{10}Be (104 atoms/g)[a]	^{10}Be exposure age (ka)	Incision rate (mm/year)	Location
1	K2-21	74.2	35.715	75.522	2433	19.84	0.93	22.1±1.5	9.0±0.6	2.2	Dassu
2	K2-42	58.7	35.732	75.665	2671	28.69	0.98	3.8±0.6	1.2±0.1	22.9	Chapok
2	K2-43	58.7	35.732	75.665	2671	28.69	0.92	2.9±0.5	0.9±0.1	29.0	
3	K2-64	44.2	35.691	75.731	2855	27.78	0.82	2.9±0.5	1.0±0.1	25.9	Pakora
4	K2-71	33.7	35.671	75.861	3010	36.09	0.76	31.1±1.0	10.8±0.3	3.3	Askole/ Biafo
5	K2-100	19.1	35.650	76.033	3215	19.24	0.99	37.7±2.7	9.0±0.4	2.0	Biafo/
5	K2-101	19.1	35.650	76.033	3215	24.01	0.97	39.1±1.1	9.5±0.2	2.7	Phanmah

Minimum ^{10}Be ages were calculated using Stone (2000) scaling factors; sea level high latitude (SLHL) production rate = 4.98 ^{10}Be atoms/g quartz per year; zero erosion rate; and sample thickness of 5 cm; asl-above sea level. Shielding factor as calculated to correct for topographic barriers using the methods of Nishiizumi et al. (1989).

[a] Atoms of ^{10}Be per gram of quartz before application of shielding correction factor.

factors were applied to compensate for the altitude-dependent effect in calculating cosmic ray exposure ages (Stone, 1999). Error range for the exposure age is shown as one standard deviation (e.g., 20 ka ± 1 σ).

3.2. Geomorphometry

The morphology of the landscape can provide insights into the interactions of surface processes and uplift (Montgomery, 1994; Safran et al., 2005). In particular, the ratio of valley width and valley height (V_f) is a useful parameter that helps to differentiate between broad-floored canyons, with relatively high V_f values (» 1), and deep boxed-shaped valleys, with relatively low V_f values (« 1) (Bull and McFadden, 1977). High values of V_f indicate the absence of the coupling of river incision and uplift. Low values of V_f reflect the coupling of river incision and uplift producing V-shaped deep valleys with streams that are actively incising, which may be associated with rapid uplift. The DEMs were used to compute distribution of hillslope angles, V_f values, and altitude-slope angle relationships for valley reaches. The DEMs with a 30-m horizontal resolution were generated from Advance Spaceborne Thermal Emission and Reflection (ASTER) images (scene #: AST_L1A.003:20000911, AST_L1A.003:20010518, AST_L1A.003:20010518, and AST_L1A.003:20000812). Slope angles were defined using a 3 × 3-point window of a best-fitting plane that was calculated to the nearest 0.1° for either side of the valley for the three reaches of the Braldu–Shigar Rivers (Fig. 2). The ~90-m size of the moving window may underestimate the real angles of the hillslope, especially in areas that have substantial curvature, such as across sharp ridges or valley bottoms. In order to determine hillslope angles for each area, ~600,000 to ~1,500,000 slope determinations were iterated and collected for the research area. The resultant slope angle distributions were sorted into 1° bins and then averaged for every 4°.

3.3. Stream power

The likely spatial changes in stream power along the Braldu River were defined by applying the stream power model of Finlayson et al. (2002). The stream power per unit area is dependent on discharge of a river and local channel slope, which were determined using the DEM that was generated from the ASTER imagery. We assumed that precipitation is uniformly supplied to the study area and we used this as for a proxy for stream discharge (Q). This assumption is valid for small basins/watershed, such as our study area, but could vary considerable over larger regions. Stream power calculations are complicated when regions are glaciated because of varying meltwater discharges between glaciers. Since the meltwater discharges for glaciers in this area are not known, we did not include a correction for possible variations in glacier discharge between glaciated catchments. However, we assumed that glacier mass balance is in dynamic equilibrium and thus the contribution of glacial discharge from each glaciated sub-basin to a river system should be equal to total annual precipitation supplied on to the sub-basins. We use these assumptions in the calculations of stream power for our study region.

4. Results

The heights and TCN surface exposure ages for the sampled strath terraces and the calculated fluvial incision rates are presented in Table 1. TCN surface exposure ages are all younger than those for glacial landforms formed during the last valley glaciation that occupied the Braldu Valley during marine oxygen isotope stage 2 (Seong et al., submitted for publication). The ages of the strath terraces range from 0.9 to 10.8 ka and are generally older with increasing height above the river. The exceptions, however, are the samples collected from the incised, gorged central reach of the Braldu River near Chapok (K2-42 and K2-43) and Pakora (K2-64). The calculated fluvial incision rates range from 2.0 to 3.3 mm/a for the lower and upper reaches, and from 22.9 to 29.0 mm/a for the gorged central reach of the Braldu River between Chapok and Pakora.

Hillslope angles for the six regions on both sides of three reaches along the Braldu and Shigar Rivers are shown in Fig. 5. The distributions of slope angles vary between the main reaches of the Braldu and Shigar Rivers. The lower reaches of the Shigar Valley (Fig. 5E and F) have a bimodal distribution of slope angles, and lower mean and mode of slope angles than the other regions. In contrast, the central gorge (Fig. 5C and D) and upper (Fig. 5A and B) reaches have unimodal distributions. The secondary peak of slope angle in the lower reach may be consistent with the distribution of alluvial fans and wide floodplains. However, the spatial distribution of slope angles shows a definitive V-shaped valley in the central reach of the Braldu Valley with relatively steep slope angles for all altitudes. (Fig. 5G). Conversely, lower and upper reaches of the Braldu and Shigar valleys exhibit lower slope angles at higher altitudes due to the influence of glaciation on the landscape.

V_f values were calculated from 11 locations (Fig. 2A) along the Braldu and Shigar Rivers. Five valley profiles were measured at the TCN sampling sites (d–d′, f–f′, g–g′, i–i′, j–j′). V_f values vary

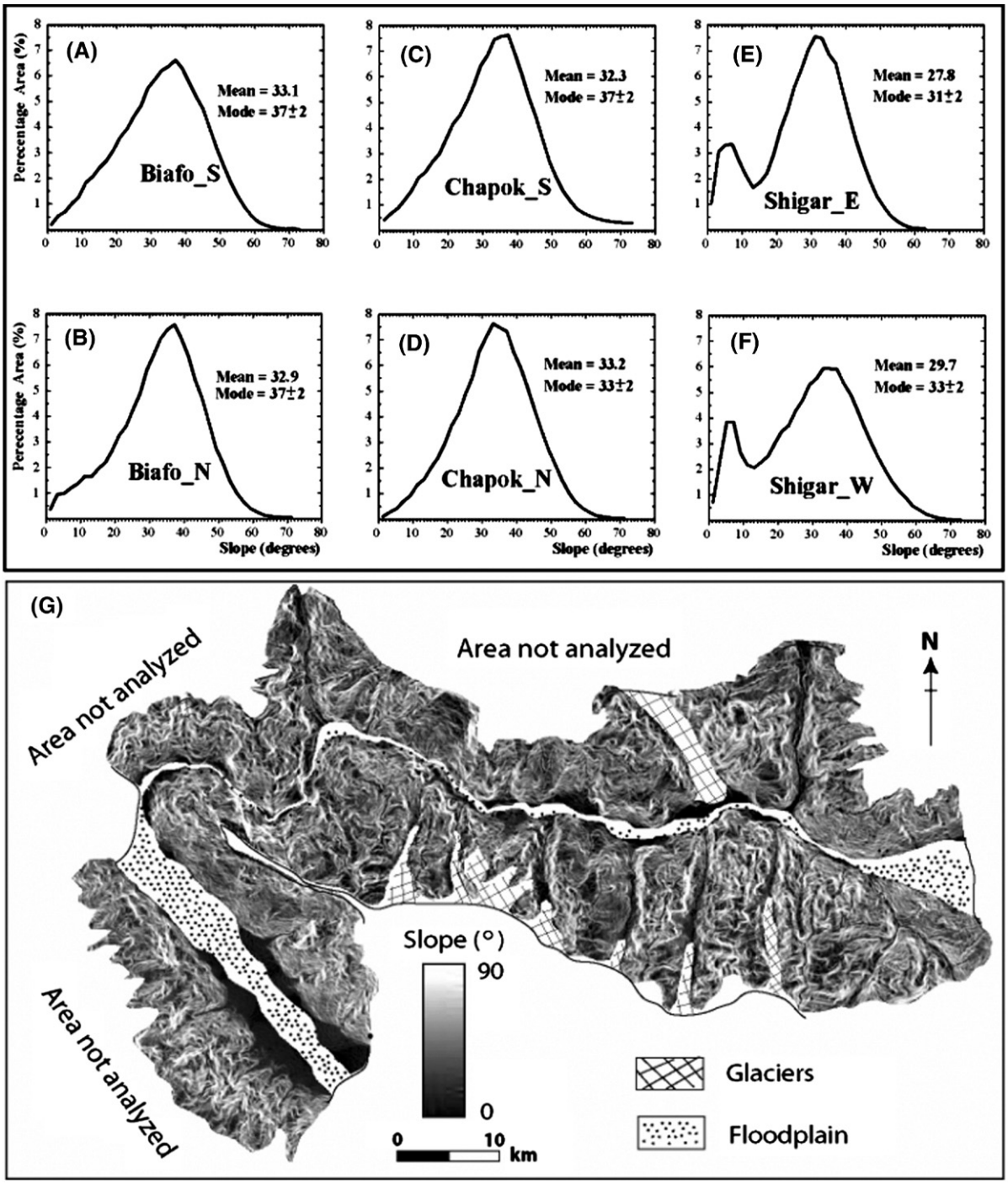

Fig. 5. Slope distributions of the basins along the Braldu–Shigar River. (A) to (F) refers to areas outlined in Fig. 2, while (G) shows the slope angles for the whole of the study area.

between the different areas: highest values were observed from the wide valley around Shigar, whereas lowest values resulted from the incised, gorged reach near Chapok (Fig. 6; Table 2). The highest values for stream power are determined for the steep, central reach of the Braldu River (Fig. 7B).

The variation of all the geomorphic metrics along the Braldu and Shigar valleys is shown in Fig. 7. The central

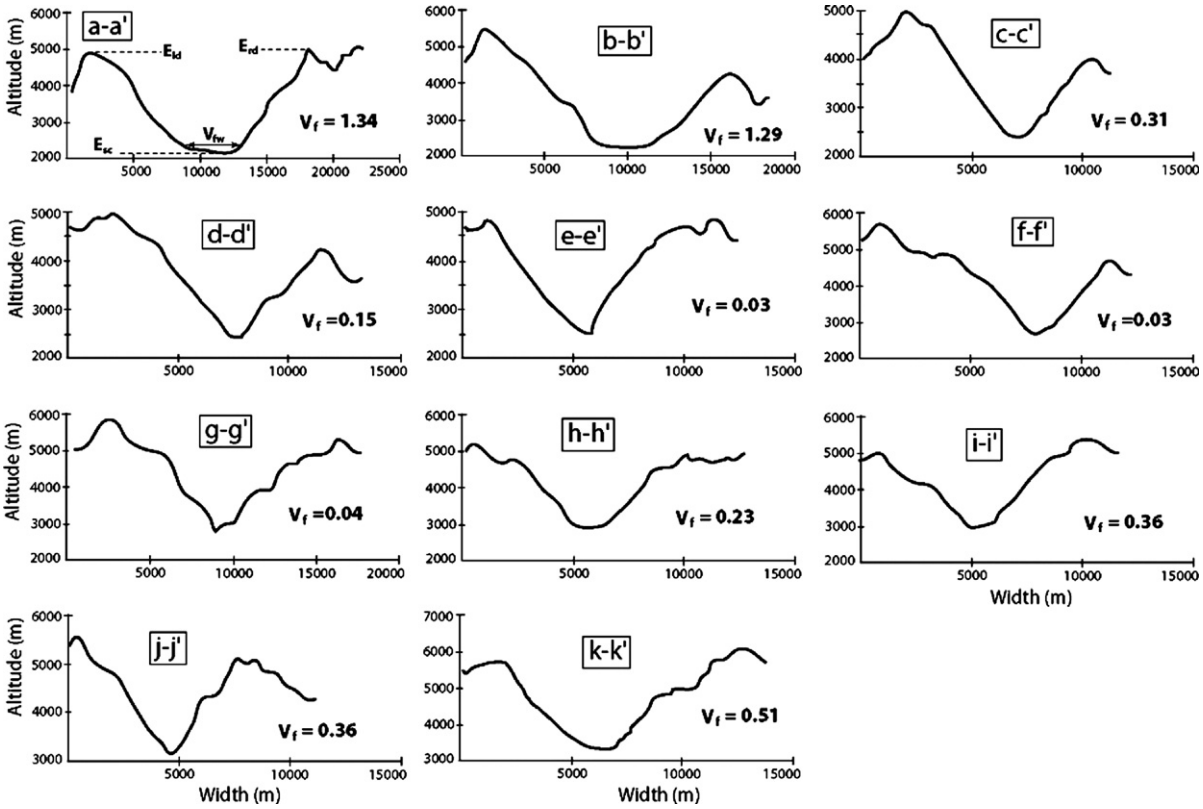

Fig. 6. Cross profiles of Braldu valley used for calculating V_f values.

reach has the highest incision rates, the lowest V_f values, relatively high slope angles with altitude, and high stream power per unit area.

5. Discussion

Valley form, river gradients, and fluvial incision rates are dependent on climate, tectonics, and surface process dynamics (Montgomery, 1994; Hartshorn et al., 2002; Roe et al., 2002; Pratt-Sitaula et al., 2004). Valley incision in this region is polygenetic and includes such processes as fluvial incision, glaciation, landsliding and debris-flow scouring. The migration of knickpoints are controlled by gradients of tributaries at confluences, the structural fabric of the bedrock, the differential rock resistance, the changes in base level, the differential bedrock uplift, and the local slope of the river bottom (Merritts et al., 1994). Therefore, interpreting stream and valley form, aggradational and entrenched alluvial fans, and changes in incision rates along a stream system is complex, but can provide a proxy for uplift when all other factors remain constant within a region.

Valley morphological conditions expressed by the DEM analysis show that the mean slope angle is ~33±2° for the gorged central reach of the river system and 28±2° for the lower and upper reaches. In addition, the modal slope angle is 37±2° for the gorged central reach and 33± 2° for the lower and upper reaches of the river system. Both sides of the Shigar River and the lowermost reach of the Braldu River (Fig. 5E and F) contain large floodplains and alluvial fans, which typically have low gradients. This

Table 2
Ratio of valley floor width to valley height (V_f)

ID	Area	V_{fw} (m)	E_{ld} (m)	E_{rd} (m)	E_{sc} (m)	V_f
a–a′	Shigar	3703	5015	4982	2235	1.34
b–b′	Mungo	3269	5440	4184	2286	1.29
c–c′	Dassu	628	4826	3990	2377	0.31
d–d′	Dassu	338	4897	4304	2389	0.15
e–e′	Chapok	73	4694	4867	2504	0.03
f–f′	Chapok	66	5697	4683	2632	0.03
g–g′	Pakora	107	5925	5369	2779	0.04
h–h′	Askole	491	5288	4832	2911	0.23
i–i′	Biafo	748	5001	5073	2947	0.36
j–j′	Panmah	773	5610	5089	3175	0.36
k–k′	Baltoro	1299	5756	6084	3366	0.51

$V_f = 2 * V_{fw}/[(E_{ld}-E_{sc})+(E_{rd}-E_{sc})]$, and V_{fw} is the width of valley floor, E_{ld} is the elevation of the left drainage divide, E_{rd} is the elevation of the right drainage divide, and E_{sc} is the elevation of the valley floor.

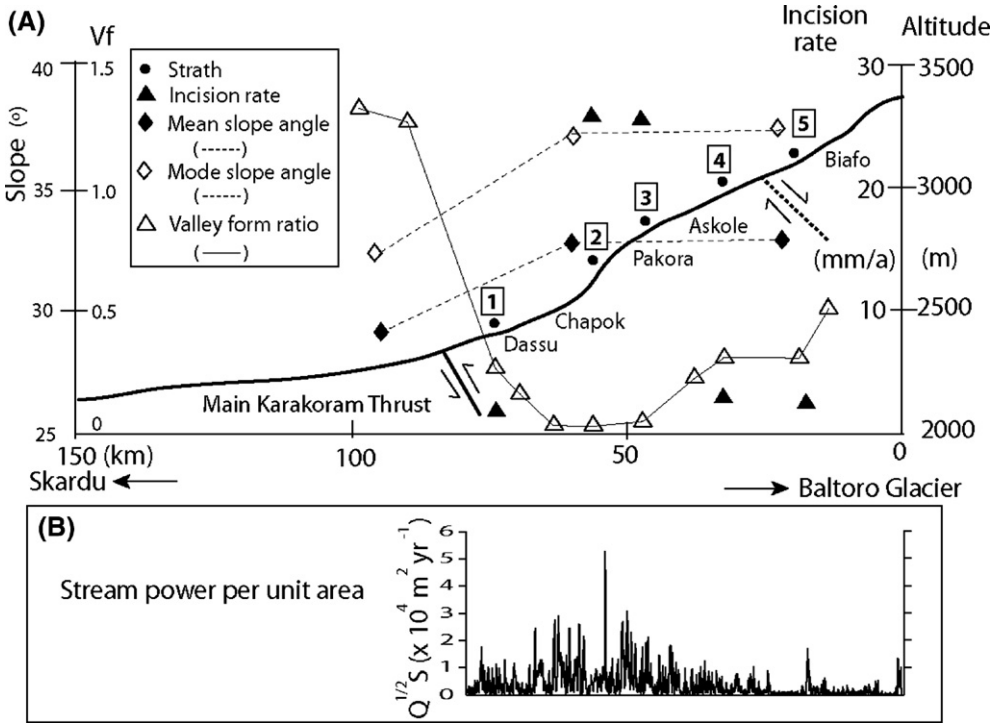

Fig. 7. (A) Slopes, ratio of valley floor width to valley height, and fluvial incision rates for the Braldu Valley plotted along longitudinal profiles. (B) Stream power per unit area along the length of the Braldu River (arranged below the longitudinal profile shown in part A) (Q — discharge of a river; S — local channel slope).

explains the second peak (at ~6°) in the frequency of slope angles. The difference in the mean and mode of slope angles between the central reach and the lower and upper reaches along the Braldu River is not significant, although the gradient of the Braldu River is significantly higher along its central gorged reach (~13 m/km compared to 4–8 m/km). Rather, the slope angles in the region are likely related to the glaciation, with the upper glaciated region (i.e. the central and upper reaches) having higher slope angles than the lower reach that is less glaciated (Seong et al., submitted for publication). Landsliding is an important hill slope process in these highly glaciated regions (Shroder, 1998; Shroder et al., in preparation), and consequently the mean slope angles are high, particularly given that most of the bedrock is extensively fractured and lacks cohesion at the hillslope scale. The high slope angles and unstable slopes produced by glacial erosion are therefore easily and rapidly modified by mass movements. In the study area, since the last glacial (after 11 ka), an equilibrium between bedrock uplift and river incision has been maintained, with hillslopes controlled by a common threshold (Burbank et al., 1996).

The lowest V_f values occur along the central gorged section of the Braldu River. Here the channel gradients are steep and incision rates are an order of magnitude higher than those for the lower and upper reaches. This difference might be due to focused uplift on the gorge central reach above the MKT and consequent rapid fluvial incision. The lower V_f values are also due to narrowing of the valley caused by valley filling owing to enhanced landsliding and sedimentation.

The strath terraces in the upper and lower reaches of the Braldu River have similar TCN surface exposure ages and heights, and consequently the incision rates are similar (2.0 to 3.3 mm/a). However, the strath terraces along the central reach has markedly younger TCN ages and the incision rates are consequently higher (22.9 to 29.0 mm/a).

The high incision rates for the gorged central reach of the Braldu River around Chapok may be the consequence of rapid incision resulting from focused tectonic uplift. The gorged central reach between Chapok and Pakora, and the main knickpoint along the Braldu River, is on the hanging wall of the Main Karakoram Thrust (MKT). This suggests that the MKT might be helping to drive enhanced uplift along the central Braldu River, with respect to the adjacent regions (Figs. 1C and 7). Furthermore, the ridge to the south of this region is experiencing active gravitational collapse resulting in the development of an impressive sackung (Shroder et al., in

preparation). This supports the view that this stretch of valley is undergoing rapid exhumation. It is possible that the knickpoint in the gorged central reach has been produced by differential uplift responding to movement of the MKT. The prominent knickpoint and the lower V_f values in the central stretch of the Braldu River help support the view of differential uplift along this stretch of the Braldu River. In other locations, such as the structural syntaxial bends at Nanga Parbat and Namche Barwa, focused fluvial incision has been found to be spatially coincident with rapid uplift by denudational unloading and weakened crust resulting in the consequent upward intrusion of mantle flow and enhanced uplift (Zeitler et al., 2001). However, we note that the river systems in the Himalayan syntaxial areas have higher discharges and have the potential to remove much larger volumes of rock over longer time periods. Furthermore, Seong et al. (submitted for publication) showed that the Braldu Valley was filled by a 1- to 2-km-thick valley glacier during glacial times, which would have likely eroded and removed significant volumes of rock, thus enhancing this denudational unloading.

We do not believe the rapid incision rates determined for the gorge section result from young TCN ages on old strath terraces that were buried by landslide debris soon after their formation and were relatively recently re-exposed by catastrophic flooding and fluvial incision and/or mass wasting. Burial by landslide debris would have shielded the strath terraces from cosmic rays reducing the production of TCNs. In the central reach, mass movements are more abundant than in the lower and upper reaches of the Braldu River, and shielding by landslide debris might occur to provide young ages and erroneously high incision rates. Furthermore, the Gomboro landslide stretches several kilometers along the valley and also occurs immediately downstream of some strath terrace sampling sites (Seong et al., in press; Shroder et al., in preparation). This landslide could have buried the strath terraces on many occasions throughout the Holocene resulting in younger TCN ages. However, the two strath terraces that were sampled in this gorge section yield similar incision rates, yet one (strath terrace #3) is outside of the landsliding zone. Furthermore, strath terrace #2, which is within the landslide zone, is in a stretch of the Braldu River that is very narrow (<50 m; Fig. 4B) and would have been rapidly incised to produce fresh bedrock surfaces as the river cut through any landslide debris and/or dam when it drained through this section.

The range of fluvial incision rates calculated for the lower and upper reaches of the study area are similar to those for other Himalayan areas, which vary from about 0.3 to 15.9 mm/a, with the majority of the rates between 2 and 6 mm/a (Burbank et al., 1996; Leland et al., 1998; Shroder et al., 1999; Barnard et al., 2001, 2004a, b, 2006; Vance et al., 2003). The fluvial incision rates for the central reach of the Braldu River are therefore very high by comparison with other studies in the Tibetan–Himalayan orogen.

The postglacial fluvial incision rate (2 to 3 mm/a) calculated from the upper and lower reaches of the Braldu River are comparable to the geologic (million year timescale) exhumation rates determined from thermochronology data for the Baltoro granite (1.2 to 1.6 mm/a; Searle et al., 1989) in the upper catchment and the Kohistan batholith (0.7 to 1.0 mm/a; Zeitler, 1985) downvalley from the study region. This shows that the fluvial incision rates are the same order of magnitude as the rock uplift rates for the uppermost reaches of the Braldu–Boltoro drainage system. However, the evidence for the higher uplift rates in the central reaches of the Braldu probably reflects differential tectonic uplift.

In summary, it is reasonable to suggest that the rapid incision along the gorged central reach of the Braldu River likely reflects a combination of focused incision, possibly resulting from tectonic forcing. The pattern of entrenched fans and the fluvial incision rate of the strath terraces along the Braldu River and its modern longitudinal profile indicate that the central reach was perhaps both tectonically uplifted and deflected by mass movement so that the Braldu River has responded through rapid downcutting.

6. Conclusion

The TCN dating along the Braldu River shows that the strath terraces formed shortly after deglaciation at ~11 ka. The rate of postglacial fluvial incision ranges from 2 to 29 mm/a. The fluvial incision rates are an order of magnitude greater in the gorged central reach of the Braldu River than the upper and lower reaches. This difference in incision rates is also reflected by the modern gradient of the longitudinal profile of the Braldu River and the V_f values, as well as by the entrenched fans. The difference in incision rates and valley morphology likely reflect the differential bedrock uplift rate of the central reach of the Braldu River above the MKT. The postglacial incision rates for the lower and upper stretches of the Braldu River are of the same order of magnitude as the exhumation rates determined from published thermochronological data for the Baltoro granite and adjacent regions.

Acknowledgements

Many thanks to Richard Marston, Marc Caffee and an anonymous reviewer for their constructive and helpful

comments on our paper. We would like to acknowledge the long-term and highly fruitful relationship with the late Syed Hamidullah, former Director of the Centre of Excellence at Peshawar University, who did so much to help us with this project. We would also like to thank his students, Faisal Khan and Mohammad Shahid, for their excellent assistance in the field. Special thanks to the medics of University of Nebraska at Omaha lead by Keith Brown and Bruce Hagen for their support in the field. This research was supported by funding from the National Geographic Society and the U.S. National Science Foundation (Grant BCS-0242339) to the University of Nebraska—Omaha and the University of Cincinnati. Part of this work was undertaken at the Lawrence Livermore National Laboratory (under DOE contract W-7405-ENG-48). This research forms part of Yeong Bae Seong's doctoral research, which was partially supported by a Meyers Fellowship at the University of Cincinnati. Special thanks to Thomas Lowell for his useful and constructive comments on an early version of this manuscript.

References

Balco, G., Stone, J.O., Lifton, N.A., Dunai, T.J., in press. A complete and easily accessible means of calculating surface exposure ages or erosion rates from ^{10}Be and ^{26}Al measurements. Quaternary Geochronology.

Barnard, P.L., Owen, L.A., Sharma, M.C., Finkel, R.C., 2001. Natural and human-induced landsliding in the Garwhal Himalaya of northern India. Geomorphology 40, 21–35.

Barnard, P.L., Owen, L.A., Finkel, R.C., 2004a. Style and timing of glacial and paraglacial sedimentation in a monsoonal influenced high Himalayan environment, the upper Bhagirathi Valley, Garhwal Himalaya. Sedimentary Geology 165, 199–221.

Barnard, P.L., Owen, L.A., Sharma, M.C., Finkel, R.C., 2004b. Late Quaternary (Holocene) landscape evolution of a monsoon-influenced high Himalayan valley, Gori Ganga, Nanda Devi, NE Garhwal. Geomorphology 61, 91–110.

Barnard, P.L., Owen, L.A., Finkel, R.C., 2006. Quaternary fans and terraces in the Khumbu Himalaya, south of Mt. Everest: their characteristics, age and formation. Journal of the Geological Society, London 163, 383–400.

Brozovic, N., Burbank, D.W., Meigs, A.J., 1997. Climatic limits on landscape development in the northwestern Himalaya. Science 276, 571–574.

Bull, W.B., McFadden, L.D., 1977. Tectonic geomorphology north and south of the Garlock Fault, California. In: Doehring, D.O. (Ed.), Geomorphology in arid regions. State University of New York, Binghamton, NY, pp. 115–138.

Burbank, D.W., Leland, J., Fielding, E., Anderson, R.S., Brozovic, N., Reid, M.R., Duncan, C., 1996. Bedrock incision, rock uplift and threshold hillslopes in the northwestern Himalayas. Nature 379, 505–510.

Finlayson, D.P., Montgomery, D.R., Hallet, B., 2002. Spatial coincidence of rapid inferred erosion with young metamorphic massifs in the Himalayas. Geology 30, 219–222.

Foster, D.A., Gleadow, A.J.W., Mortimer, G., 1994. Rapid Pliocene exhumation in the Karakoram (Pakistan), revealed by fission-track thermochronology of the K2 gneiss. Geology 22, 19–22.

Hartshorn, K., Hovius, N., Dade, W.B., Slingerland, R.L., 2002. Climate-driven bedrock incision in an active mountain belt. Science 297, 2036–2038.

Hewitt, K., 1998. Catastrophic landslides and their effects on the Upper Indus streams, Karakoram Himalaya, northern Pakistan. In: Shroder, Jr., J.F. (Ed.), Mass Movement in the Himalaya. Geomorphology, vol. 26, pp. 47–80.

Kirby, E., Whipple, K., 2001. Quantifying differential rock-uplift rates via stream profile analysis. Geology 29, 415–418.

Kohl, C.P., Nishiizumi, K., 1992. Chemical isolation of quartz for measurement of in-situ produced cosmogenic nuclides. Geochimica et Cosmochimica Acta 56, 3583–3587.

Lal, D., 1991. Cosmic ray labeling of erosion surfaces: in situ nuclide production rates and erosion models. Earth and Planetary Science Letters 104, 429–439.

Leland, J., Reid, M.R., Burbank, D.W., Finkel, R., Caffee, M., 1998. Incision and differential bedrock uplift along the Indus River near Nanga Parbat, Pakistan Himalaya, from ^{10}Be and ^{26}Al exposure age dating of straths. Earth and Planetary Science Letters 154, 93–107.

Merritts, D.J., Vincent, K.R., Wohl, E.E., 1994. A guide to interpreting fluvial terraces. Journal of Geophysical Research 99 (B7), 14031–14050.

Montgomery, D.R., 1994. Valley incision and uplift of mountain peaks. Journal of Geophysical Research 99 (B7), 13913–13921.

Montgomery, D.R., 2004. Observations on the role of lithology in strath terrace formation and bedrock channel width. American Journal of Science 304, 454–476.

Montgomery, D.R., Finnegan, N., Anders, A., Hallet, B., 2002. Downstream adjustment of channel width to spatial gradients in rates of rock uplift at Namche Barwa. GSA Annual Meeting Abstract 34 (6), 241.

Nishiizumi, K., Imamura, M., Caffee, M.W., Southon, J.R., Finkel, R.C., McAninch, J., 2007. Absolute calibration of ^{10}Be AMS Standards. Nuclear Instruments and Methods B 258, 403–413.

Nishiizumi, K., Winterer, E.L., Kohl, C.P., Lal, D., Arnold, J.R., Klein, J., Middleton, R., 1989. Cosmic ray production rates of ^{10}Be and ^{26}Al in quartz from glacially polished rocks. Journal of Geophysical Research 94(B12), 17907–17915.

Parrish, R.R., Tirrul, R., 1989. U–Pb age of the Baltoro granite, northwest Himalaya, and implications for monazite U–Pb systematics. Geology 17, 1076–1079.

Pratt-Sitaula, B., Burbank, D., Heimsath, A., Ojha,, 2004. Landscape disequilibrium on 1000–10,000 year scales Marsyandi River, Nepal, central Himalaya. Geomorphology 58, 223–241.

Robinson, A.C., Yin, A., Manning, C.E., Harrison, T.M., Zhang, S.H., Wang, X.F., 2004. Tectonic evolution of the north eastern Pamir: constraints from the portion of the Cenozoic Kongur Shan extensional system, western China. Geological Society of America Bulletin 116, 953–973.

Roe, G.H., Montgomery, D.R., Hallet, B., 2002. Effects of orographic precipitation variations on the concavity of steady-state river profiles. Geology 30, 143–146.

Safran, E.B., Bierman, P.R., Aalto, R., Dunne, T., Whipple, K.X., Caffee, M., 2005. Erosion rates driven by channel network incision in the Bolivian Andes. Earth Surface Processes and Landforms 30, 1007–1024.

Searle, M.P., 1991. Geology and tectonics of the Karakoram Mountains. John Wiley and Sons, Chichester, UK.

Searle, M.P., Rex, A.J., Tirrul, R., Rex, D.C., Barnicoat, A., 1989. Metamorphic, magmatic and tectonic evolution of the central Karakoram in the Biafo–Baltoro–Hushe regions of N. Pakistan. In: Malinconico, L.L., Lillie, R.S. (Eds.), Geology and Tectonics of the Western Himalaya. Geological Society of America Special Publication, vol. 232. Geological Society of America, Boulder, Colorado, pp. 47–73.

Seeber, L., Gornitz, V., 1983. River profiles along the Himalayan arc as indicators of active tectonics. Tectonophysics 92, 335–367.

Seong, Y.B., Bishop, M., Bush, A., Copeland, L., Finkel, R.C., Kamp, U., Owen, L.A., Shroder, J.F., in press. Landforms and landscape evolution in the Skardu, Braldu and Shigar Valleys, Central Karakoram Mountains. Geomorphology.

Seong, Y.B., Owen, L.A., Bishop, M., Bush, A., Copeland, L., Finkel, R.C., Kamp, U., Shroder, J.F., submitted for publication. Quaternary glacial history of the Central Karakoram. Quaternary Science Review.

Shroder Jr., J.F., 1998. Slope failure and denudation in the western Himalaya. Geomorphology 26, 81–105.

Shroder, J.F., Scheppy, R.A., Bishop, M.P., 1999. Denudation of small alpine basins, Nanga Parbat Himalaya, Pakistan. Arctic, Antarctic, and Alpine Research 31, 121–127.

Shroder, J., Bishop, M., Bush, A., Copeland, L., Kamp, U., Owen, L.A., Seong, Y.B., Weeks, P., in preparation. Postglacial slope failure and denudation in the Central Karakoram.

Stone, J.O., 1999. A consistent Be-10 production rate in quartz — muons and altitude scaling. AMS-8 Proceedings Abstract Volume, Vienna, Austria.

Stone, J.O., 2000. Air pressure and cosmogenic isotope production. Journal of Geophysical Research 105 (B10), 23753–23759.

Vance, D., Bickle, M., Ivy-Ochs, S., Kubik, P.W., 2003. Erosion and exhumation in the Himalaya from cosmogenic isotope inventories of river sediments. Earth and Planetary Science Letters 206, 273–288.

Zeitler, P.K., 1985. Cooling history of the NW Himalaya. Tectonics 4, 127–151.

Zeitler, P.K., Meltzer, A.S., Koons, P.O., Craw, D., Hallet, B., Chamberlain, C.P., Kidd, W.S.F., Park, S.K., Seeber, L., Bishop, M.P., Shroder, J., 2001. Erosion, Himalayan geodynamics, and the geomorphology of metamorphism. GSA Today 11, 4–9.

Zhang, D.D., 1998. Geomorphological problems of the middle reaches of the Tsangpo River, Tibet. Earth Surface Processes and Landforms 23, 889–903.